

Deformation Monitoring of Shuangwangcheng Reservoir Based on Time-Series InSAR Method

Guanghui Zhang
College of Resources
Shandong University of Science and Technology
Taian, China
202283300014@sdust.edu.cn

Zhuopu Zhang
College of Resources
Shandong University of Science and Technology
Taian, China
202283300016@sdust.edu.cn

Yuntao Zhang
Shandong Provincial Institute of Land Surveying and Mapping
Jinan, China
tonyzyt@163.com

* Zhigang Yu
College of Resources
Shandong University of Science and Technology
Taian, China
* Corresponding author: yu_zg@sdust.edu.cn

Wei Jiang
Tai'an Engineering Construction Guidance Service Center
Taian, China
13515486185@163.com

Abstract—To conduct an investigation on the deformation of the Shuangwangcheng Reservoir, this study employed the full-resolution time-series InSAR method to analyze the Sentinel-1 ascending and descending track data from July 2015 to July 2023. The investigation unveiled substantial subsidence in the reservoir dam, exhibiting deformation rates varying from -15 mm/year to -30 mm/year. Notably, a disparity in subsidence rates was observed between the eastern and western sides of the reservoir. Subsequently, the SBAS-InSAR method was employed to monitor the deformation of the surrounding area of the reservoir. It was revealed that the differential deformation rate of the dam may be attributed to the extraction of underground brine from the salt field located on the eastern side of the reservoir.

Keywords-subsidence; InSAR; full-resolution; saltwork

I. INTRODUCTION

Surface deformation, being a widespread geological hazard, presents a substantial risk to the reliable functioning of human-made infrastructure. Surface deformation has a significant impact on various types of infrastructure, including roads, bridges, and dams, rendering them vulnerable to structural damage such as cracking and tilting. Embracing advanced technology is of utmost importance in the monitoring and prevention of surface deformation. Interferometric Synthetic Aperture Radar (InSAR) technology obviates the necessity for on-site measurements, resulting in substantial reductions in labor expenses, while also offering a significantly greater density of deformation monitoring points in comparison to leveling and GNSS measurements [1,2]. This development presents novel opportunities for the monitoring of surface deformation.

Persistent Scatterer Interferometric Synthetic Aperture (PS-InSAR) and Small Baseline Subset Interferometric Synthetic Aperture (SBAS-InSAR) are two widely employed time-series InSAR techniques that have significant implications in the monitoring of surface deformation [3]. The PS-InSAR method provides a high level of resolution and accuracy. However, its applicability is limited to urban areas characterized by a dense distribution of permanent scatterers [4]. On the contrary, the SBAS-InSAR method employs multilook filtering to acquire a more extensive range of deformation data. However, it is important to note that this method exhibits lower monitoring accuracy and resolution when compared to the PS-InSAR method [5]. The application of InSAR methods for deformation monitoring poses significant challenges when it comes to monitoring targets like reservoir dams. These dams typically have widths that vary from a few meters to tens of meters and are commonly situated in non-urban areas.

Combining permanent scatterers with distributed scatterers can significantly enhance the deformation monitoring capability of the PS-InSAR method [6]. This integration enables the achievement of full-resolution time-series InSAR monitoring of elongated targets in non-urban areas. However, a limitation of this approach is the need for substantial computational resources, which poses a challenge when attempting to implement it for monitoring large-scale deformations. To tackle this issue, we propose a hybrid approach that combines the full-resolution time-series InSAR method with the SBAS-InSAR method. The full-resolution time-series InSAR method is employed to acquire high-resolution deformation data within a limited area of interest, whereas the SBAS-InSAR method is utilized to capture the broader-scale deformation information encompassing the target region. By conducting a comprehensive analysis of these

datasets, valuable insights can be obtained regarding the patterns of deformation in the study region.

In this study, the Sentinel-1 data spanning from July 2015 to July 2023 were utilized for the purpose of monitoring the deformation of the Shuangwangcheng Reservoir. The full-resolution time-series InSAR method is utilized for the purpose of monitoring the deformation occurring within the reservoir area. Additionally, the SBAS-InSAR method is employed for the purpose of monitoring the deformation occurring in the reservoir and its adjacent regions. Finally, a comprehensive analysis is conducted on the deformation characteristics of the reservoir dam and the factors that influence such deformation. This study offers empirical evidence and a theoretical framework to comprehend the deformation condition of the Shuangwangcheng Reservoir dam.

II. RESEARCH AREA AND DATA

A. Study Area

The Shuangwangcheng Reservoir is located in the municipality of Weifang, which is part of the province of Shandong. The reservoir plays a crucial role in the storage of water for the South-to-North Water Diversion Project. The Shuangwangcheng Reservoir dam possesses a vertical elevation of 12.5 m and spans a total length of 9.6 km along its dam axis. The existing Shuangwangcheng Reservoir was rebuilt on the basis of the original reservoir and completed in June 2013. The geographical depiction of the Shuangwangcheng Reservoir is illustrated in Fig 1.

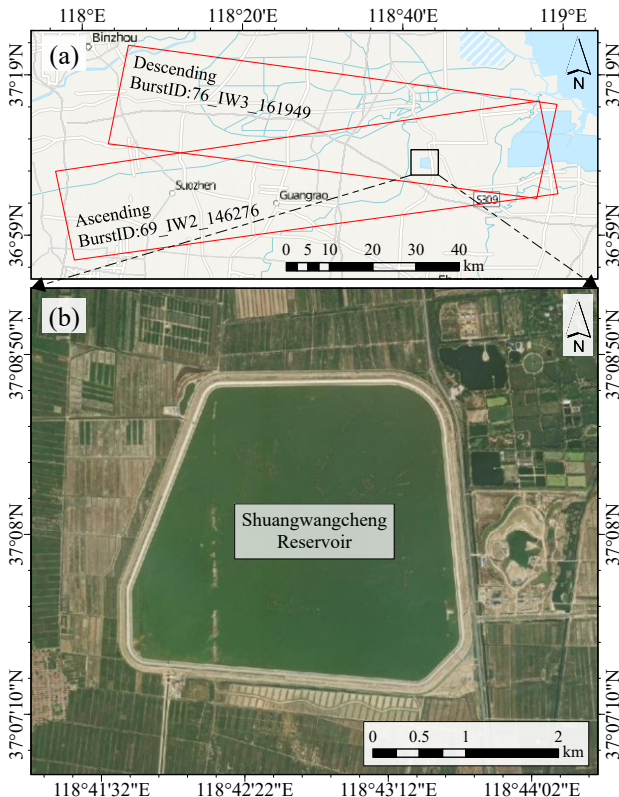


Figure 1. Location of the study area. (a) represents burst coverage area and reservoir location, (b) is a satellite image of the reservoir.

B. Data

The study selected image data acquired by the Sentinel-1 satellite at Shuangwangcheng Reservoir from July 1, 2015, to July 31, 2023. Currently, the Sentinel-1 satellite constellation comprises two satellites, namely A and B. Each individual satellite has a revisit period of 12 days, while the combined A and B satellites achieve a minimum revisit period of 6 days. The satellite carries a C-band synthetic aperture radar with a signal wavelength of 5.6 cm. The data obtained from these satellites has a spatial resolution of 5 m × 20 m (range × azimuth).

A total of 408 images were chosen, including 260 ascending track images and 148 descending track images. The available ascending track image data spans from July 1, 2015 to July 31, 2023, while the available descending track image data spans from July 1, 2015 to December 14, 2021. The burst ranges and numbering of the selected image data are illustrated in Fig 1(a). The distribution of ascending and descending images for the selected Shuangwangcheng Reservoir area over the years is shown in Fig 2.

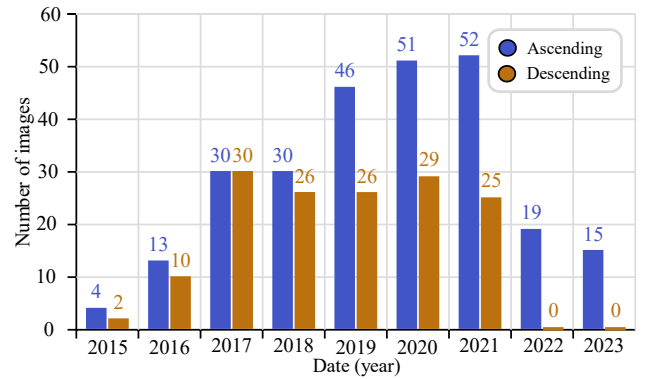


Figure 2. Image quantity distribution. No descending track data since 2022.

III. TIME-SERIES INSAR METHOD

A. Method

This study employed a full-resolution time-series InSAR method that combines persistent scatterers and distributed scatterers. The key lies in the selection of homogeneous points and the utilization of their statistical characteristics to optimize the phase of distributed scatterers, thereby mitigating the influence of phase noise. This method sacrifices a significant amount of computation time in exchange for the accuracy and density of deformation monitoring results. To enhance computational efficiency, this study initially focused on deformation monitoring solely in the reservoir area, utilizing the full-resolution time-series InSAR method. Subsequently, SBAS-InSAR method was employed to monitor the areas surrounding the reservoir.

B. Process

1) Coregistration

The 260 ascending track images and the 148 descending track images should be coregistered separately, and the ISCE software should be utilized to accomplish this task [7]. Then, crop the registered data to the Shuangwangcheng Reservoir area.

2) Phase Linking

In this step, the complete network of wrapped phases is phase linking based on the Eigendecomposition-based Maximum-likelihood-estimator of Interferometric phase (EMI) method, and the Statistically Homogeneous Pixels (SHPs) are selected based on the Kolmogorov-Smirnov test (KS) method. This step is computationally intensive and time-consuming. This step is done using MiaplPy [8].

3) Select Image Pairs

The conventional method for selecting image pairs is the single master image approach. This method assumes the presence of N scene images and involves selecting one of the scene images as the master image. Interfering image pairs are then formed by pairing the master image with each of the remaining N-1 images. This approach leads to decoherence as a consequence of the significant time gap between certain pairs of images. Given that the duration of the selected images in this study spans 8 years, the Delaunay network is employed to choose pairs of images. This method ensures that image pairs with shorter temporal and spatial baselines are selected in an optimal manner. The formed image pairs are depicted in Fig 3 and Fig 4.

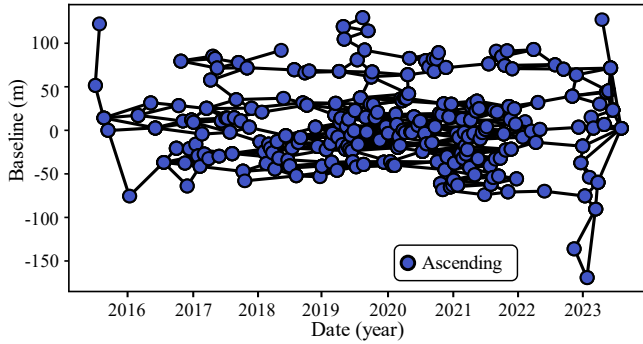


Figure 3. Network of ascending track images. From July 2015 to July 2023.

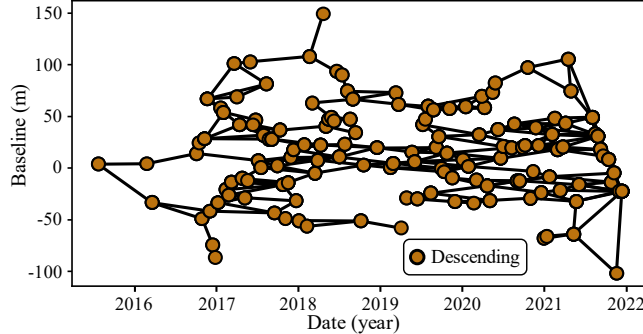


Figure 4. Network of descending track images. From July 2015 to December 2021.

4) Interference and Unwrapping

Interferometric processing is performed on the phase linking optimised image pairs to generate interferograms. The interferograms are input to SNAPHU for phase unwrapping processing to generate unwrapped phase images.

5) Time Series Processing

The L1-norm minimisation method was used to perform time series inversion of the unwrapped phase data in order to generate the final time series deformation results, after which the results were encoded from under the radar coordinate system to under the geographic coordinate system.

6) Extension Area

In order to analyse the recent wide-area deformation information in the peripheral region of the reservoir, this study simultaneously monitored the deformation of the peripheral region of the reservoir by the conventional SBAS-InSAR method. The Sentinel-1 ascending track images between January 2022 and July 2023 were selected, and the multilook parameters were set to 10×2 (range \times azimuth), with a spatial baseline threshold of 200 m and a temporal baseline threshold of 60 days. Interferograms were generated through the HyP3 online service [9], followed by time-series processing using MintPy to generate the final deformation results [10].

IV. RESULTS AND DISCUSSION

After applying the full-resolution time-series InSAR technique, deformation data derived from both ascending and descending tracks were acquired. The results obtained provide deformation data in the line-of-sight direction of the satellite radar. A reference point was chosen at a building area located on the northwest side of reservoir, as shown in Fig 5 and Fig 6.

The deformation rate map derived from the ascending track data is presented in Fig 5. The rate at which the dam sinks exceeds the rate at which the perimeter of the dam sinks. The rate of subsidence is higher on the eastern side of the reservoir in comparison to the western side. The subsidence rate in the reservoir area reaches a maximum of 31 mm/year.

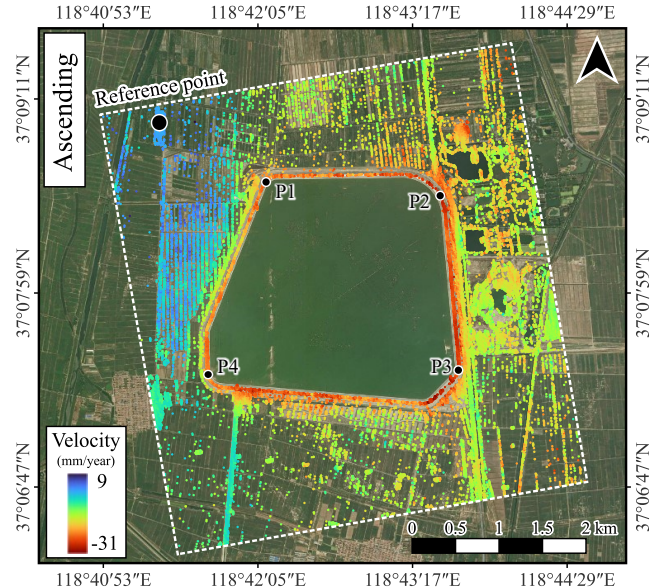


Figure 5. Deformation rate by ascending. From July 2015 to July 2023.

The deformation rate map derived from the data collected during the descending track is presented in Fig 6. The deformation characteristics depicted in this map exhibit a high degree of consistency with the deformation rate map derived

from the data obtained from the ascending track. The subsidence rate is observed to be higher on the eastern side in comparison to the western side, and the dam exhibits a greater subsidence rate when compared to the surrounding area.

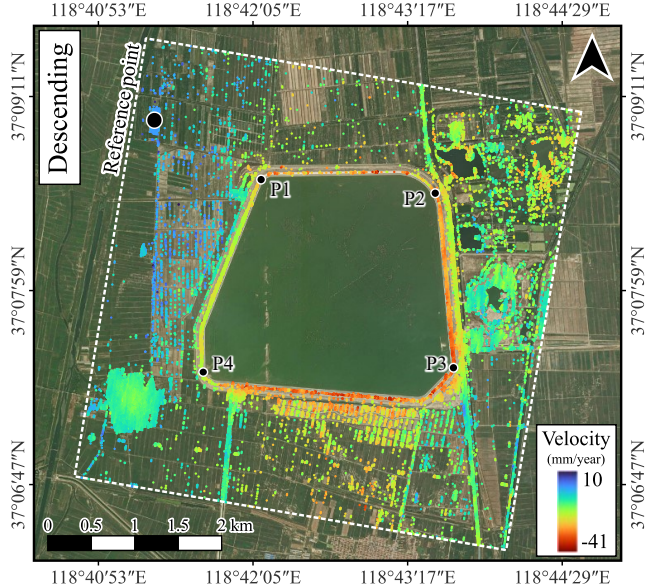


Figure 6. Deformation rate by descending. From July 2015 to December 2021.

Four points, denoted as P1 to P4, were strategically chosen along the reservoir dam in order to construct a time-series deformation graph. The selected points are shown in Fig 5 and Fig 6. The time-series data of these points was analyzed by fitting a quadratic polynomial. The resulting fitted lines were used to generate the time-series deformation graph, as shown in Fig 7. The reservoir dam has been settling during the monitoring period.

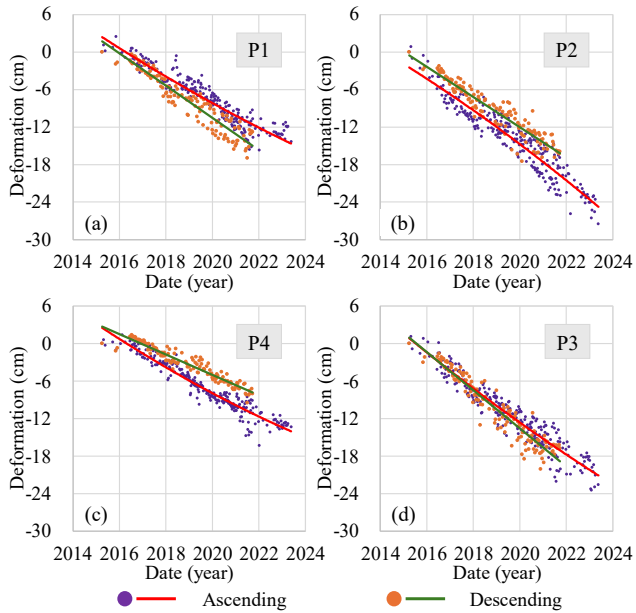


Figure 7. Time series deformation. (a) to (d) represents the temporal deformation of each point.

There exists a notable disparity in deformation patterns between the western region of the reservoir, where P1 and P4 are situated, and the eastern region, where P2 and P3 are situated. The difference in deformation between P2 and P4 has already exceeded 10 cm.

Starting from P1, the deformation rate curve is plotted along the reservoir dam in a clockwise direction with a sampling interval of 50 m. The deformation rate curve is shown in Fig 8. It should be noted that the inconsistent monitoring of the line direction on the ascending and descending tracks is one of the reasons for the difference in deformation rate between them. In addition, there are fewer images for the descending track data, and there is no descending track data between 2022 and 2023. Therefore, subsequent analysis will mainly focus on the ascending track data. The deformation rates in the western section of the reservoir dam (from point P2 to P3) are primarily concentrated between -20 mm/year and -30 mm/year. The deformation rates in the eastern section of the reservoir dam (from point P4 to P1) are mainly concentrated between -15 mm/year and -25 mm/year.

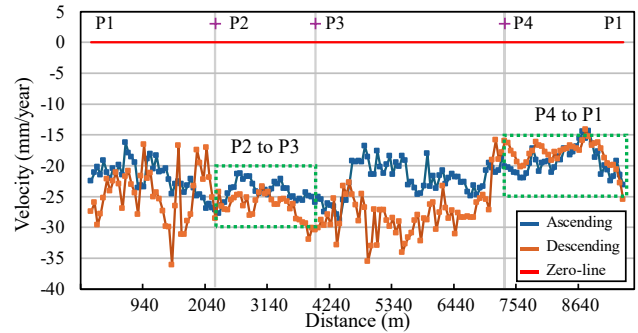


Figure 8. Deformation rate along the reservoir dam. The settlement rate is determined along the axis of the dam.

The deformation map of the reservoir and its surrounding areas, generated using the SBAS-InSAR method, is shown in Fig 9. The map shows significant deformation extending from the reservoir to the east and reaching the coastal area. The center of the subsidence funnel in Yanyuan Saltwork is situated 4.5 km away from the reservoir, as shown in Fig 9 and Fig 10.

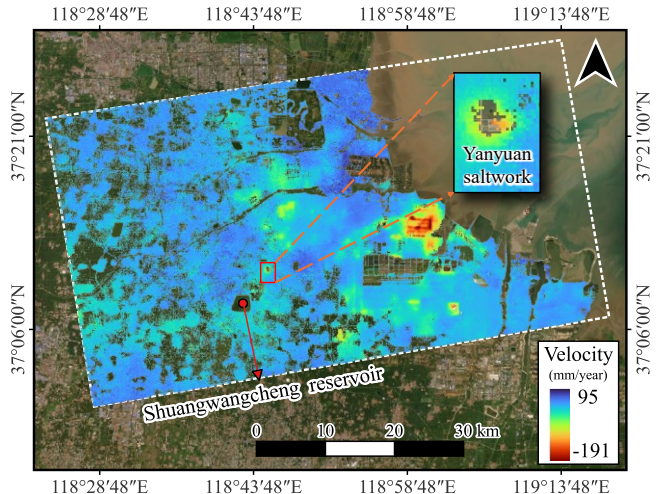


Figure 9. Deformation rate by SBAS-InSAR. From January 2022 to July 2023.

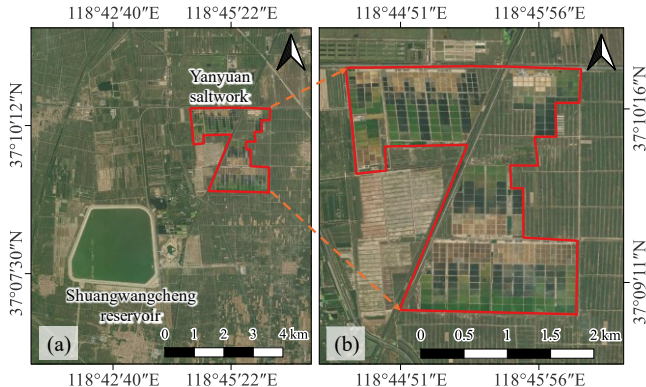


Figure 10. Location of reservoir and saltwork. (a) Location of the saltwork, (b) Satellite images of the saltwork.

According to previous studies, there is a correlation between reservoir water level changes and dam deformation [2]. In addition, changes in reservoir water level can cause different degrees of seepage, which ultimately affects the overall stability of the dam structure. The salt industry in the Shuangwangcheng area has an important historical background, and the existence of a large number of salt fields has an impact on the groundwater level. Through the analysis of 8 years of deformation monitoring data, it was found that there is obvious plastic deformation in the dam body of the reservoir. This deformation may be formed by a variety of factors, such as fluctuations in the reservoir water level, seepage phenomena, and changes in the groundwater level.

The Yanyuan Saltwork located on the northeast side of the reservoir extracts a significant quantity of subterranean brine for salt production. This activity has resulted in alterations in the groundwater level, potentially leading to uneven settlement of the reservoir. The discrepancy in subsidence rates between the eastern and western sides of the reservoir can cause uneven stress distribution, potentially resulting in dam deformation and cracking. This issue requires more attention than the overall subsidence.

V. CONCLUSIONS

This study is based on the full-resolution time-series InSAR method to process the ascending and descending track data. It aims to identify and verify the deformation characteristics of the Shuangwangcheng Reservoir. It confirms that the reservoir dam experiences significant subsidence, with higher rates of deformation on the eastern side compared to the western side. The deformation results obtained from the ascending and descending data have high consistency, which indicates that this method is suitable for the deformation monitoring of reservoir dam. From July 2015 to July 2023, the deformation rate in the eastern side ranged from -20 mm/year to -30 mm/year, while in the western side, it ranged from -15 mm/year to -25 mm/year. Combining the results of the SBAS-InSAR method, it is observed that there is extensive subsidence in the saltwork area on the eastern side of the reservoir. The underground brine extraction from the saltwork on the east side of the reservoir may be the cause of the difference in the deformation rate of the reservoir. This study establishes a solid scientific foundation for preventing geological hazards and managing water resources.

ACKNOWLEDGMENTS

This work was supported in part by the Taian Science and Technology Innovation Development Project (NO. 2022GX087).

REFERENCES

- [1] Aswathi, J., Kumar, R.B., Oommen, T., Bouali, E.H. and Sajinkumar, K.S. (2022) InSAR as a tool for monitoring hydropower projects: A review. Energy Geoscience, 3(2), pp.160-171.
- [2] Xiao, R., Shi, H., He, X., Li, Z., Jia, D. and Yang, Z. (2019) Deformation monitoring of reservoir dams using GNSS: An application to south-to-north water diversion project, China. IEEE Access, 7, pp.54981-54992.
- [3] Zheng, Z., Xie, C., He, Y., Zhu, M., Huang, W. and Shao, T. (2022) Monitoring potential geological hazards with different InSAR algorithms: The case of western Sichuan. Remote Sensing, 14(9), p.2049.
- [4] Ramirez, R.A., Lee, G.J., Choi, S.K., Kwon, T.H., Kim, Y.C., Ryu, H.H., Kim, S., Bae, B. and Hyun, C. (2022) Monitoring of construction-induced urban ground deformations using Sentinel-1 PS-InSAR: The case study of tunneling in Daegu, Korea. International Journal of Applied Earth Observation and Geoinformation, 108, p.102721.
- [5] Li, S., Xu, W. and Li, Z. (2022) Review of the SBAS InSAR Time-series algorithms, applications, and challenges. Geodesy and Geodynamics, 13(2), pp.114-126.
- [6] Ferretti, A., Fumagalli, A., Novali, F., Prati, C., Rocca, F. and Rucci, A. (2011) A new algorithm for processing interferometric data-stacks: SqueezSAR. IEEE transactions on geoscience and remote sensing, 49(9), pp.3460-3470.
- [7] Fattah, H., Agram, P. and Simons, M. (2016) A network-based enhanced spectral diversity approach for TOPS time-series analysis. IEEE Transactions on Geoscience and Remote Sensing, 55(2), pp.777-786.
- [8] Mirzaee, S., Amelung, F. and Fattah, H. (2023) Non-linear phase linking using joined distributed and persistent scatterers. Computers & geosciences, 171, p.105291.
- [9] Agapiou, A. and Lysandrou, V. (2020) Detecting displacements within archaeological sites in Cyprus after a 5.6 magnitude scale earthquake event through the hybrid pluggable processing pipeline (HyP3) cloud-based system and sentinel-1 interferometric synthetic aperture radar (InSAR) analysis. IEEE Journal of Selected Topics in Applied Earth Observations and Remote Sensing, 13, pp.6115-6123.
- [10] Yunjun, Z., Fattah, H. and Amelung, F. (2019) Small baseline InSAR time series analysis: Unwrapping error correction and noise reduction. Computers & Geosciences, 133, p.104331.